

University of Groningen

Application of the Maxwell-Stefan theory to the transport in ion-selective membranes used in the chloralkali electrolysis process

Stegen, J.H.G. van der; Veen, A.J. van der; Weerdenburg, H.; Hogendoorn, J.A.; Versteeg, G.F.

Published in:
Chemical Engineering Science

DOI:
[10.1016/S0009-2509\(98\)00465-5](https://doi.org/10.1016/S0009-2509(98)00465-5)

IMPORTANT NOTE: You are advised to consult the publisher's version (publisher's PDF) if you wish to cite from it. Please check the document version below.

Document Version
Publisher's PDF, also known as Version of record

Publication date:
1999

[Link to publication in University of Groningen/UMCG research database](#)

Citation for published version (APA):

Stegen, J. H. G. V. D., Veen, A. J. V. D., Weerdenburg, H., Hogendoorn, J. A., & Versteeg, G. F. (1999). Application of the Maxwell-Stefan theory to the transport in ion-selective membranes used in the chloralkali electrolysis process. *Chemical Engineering Science*, 54(13), 2501-2511. [https://doi.org/10.1016/S0009-2509\(98\)00465-5](https://doi.org/10.1016/S0009-2509(98)00465-5)

Copyright

Other than for strictly personal use, it is not permitted to download or to forward/distribute the text or part of it without the consent of the author(s) and/or copyright holder(s), unless the work is under an open content license (like Creative Commons).

The publication may also be distributed here under the terms of Article 25fa of the Dutch Copyright Act, indicated by the "Taverne" license. More information can be found on the University of Groningen website: <https://www.rug.nl/library/open-access/self-archiving-pure/taverne-amendment>.

Take-down policy

If you believe that this document breaches copyright please contact us providing details, and we will remove access to the work immediately and investigate your claim.

Downloaded from the University of Groningen/UMCG research database (Pure): <http://www.rug.nl/research/portal>. For technical reasons the number of authors shown on this cover page is limited to 10 maximum.



Application of the Maxwell–Stefan theory to the transport in ion-selective membranes used in the chloralkali electrolysis process

J.H.G. van der Stegen^a, A.J. van der Veen^b, H. Weerdenburg^c, J.A. Hogendoorn^{d,*},
G.F. Versteeg^d

^a*AKZO-Nobel Central Research B.V., RTB department, P.O. Box 9300, 6800 SB SB Arnhem, Netherlands*

^b*Shell, P.O. Box 6060, 4780 LN, Moerdijk, Netherlands*

^c*Tebodin, P.O. Box 1133, 1940 EC, Beverwijk, Netherlands*

^d*University of Twente, P.O. Box 217, 7500 AE Enschede, Netherlands*

Abstract

The results of a fundamental mass transport model based on the Maxwell–Stefan approach are compared to experimental data obtained by Akzo-Nobel for a Dupont Nafion ion-selective membrane as used in chloralkali electrolysis processes. The main problem in the application of the Maxwell–Stefan based mass transfer model to the chloralkali electrolysis process is a lack of available diffusivities for the membrane. Estimation of these diffusivities in the membrane based on a method presented by Wesselingh et al. (1995. *Chem. Engng J.*, 57, 75–89) gave unrealistic high membrane potential drops. Therefore, another method was followed. First, a sensitivity analysis was carried out which resulted in a reduced set consisting of the dominating Maxwell–Stefan diffusivities. First estimates of these remaining diffusivities were determined for single layer sulfonic and a carboxylic membranes. With a slight adjustment of the values of the diffusivities obtained for the separate sulfonic and carboxylic layers, the performance parameters of the DuPont Nafion membrane could be predicted well for a reference experiment. These diffusivities also proved to be suitable for other anolyte strengths. However, for other catholyte strengths and current densities these diffusivities (even after a correction for the water uptake according to the method of Wesselingh et al. (1995. *Chem. Engng. J.*, 57, 75–89)) did not result in a good agreement between the simulated and experimentally observed performance parameters. Only after a correction of the diffusivities the simulations yielded approximately the same performance parameters as experimentally observed. From this it can be concluded that although a fundamental model is used in order to describe the mass transfer in a membrane, a single set of diffusivities is not sufficient in order to obtain the experimentally observed performance parameters at different process conditions. At this moment there is not enough knowledge on the exact phenomena taking place in the membrane in order to predict the necessary corrections of the diffusivities a priori. As long as there are no theoretically founded and reliable relations available to predict the Maxwell–Stefan diffusivities in a membrane (or accurate experimental data for these diffusivities) only a semi-empirical method as used in this study can serve as a basis for a further progress in the development of an existing (in this case DuPont Nafion) membrane. © 1999 Elsevier Science Ltd. All rights reserved.

Keywords: Mass transport; Maxwell–Stefan; Membrane; Chloralkali electrolysis; Nafion

1. Introduction

Chlorine is produced by the chloralkali electrolysis process which uses NaCl as raw material. The indus-

trially used electrolysis cells are the mercury, the diaphragm and the membrane cell. Owing to environmental and economical reasons, an increasing amount of the required chlorine is nowadays produced by the relatively new membrane processes. Already in 1983, Akzo-Nobel was one of the first companies in Europe to operate this new membrane electrolysis process. In these processes the cathode and the anode compartment in the electrolysis cell are separated by a cat-ion selective membrane of

*Corresponding author. Tel.: 0031 53 489 4337; fax: 0031 53 489 4774; e-mail: kees.hogendoorn@wxs.nl.

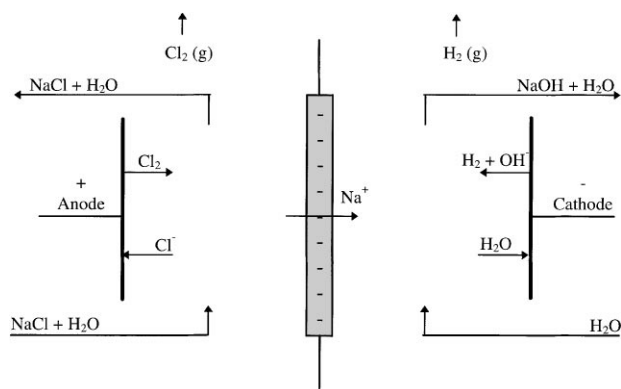


Fig. 1. Schematic representation of a cell unit in the chloralkali process.

about 50–200 μm thickness. The anode compartment is fed with a brine solution (a typical concentration in the anode compartment is about 180–200 g/l NaCl, pH ranges from 1 to 4.5). At the anode chloride ions are converted to gaseous chlorine. The cathode compartment is fed with water and at the cathode water is transferred into gaseous hydrogen and hydroxyl ions. The sodium ions diffuse and migrate through the cation selective membrane from the anode to the cathode compartment. Combined with the hydroxyl ions, sodium leaves the membrane cell as sodium hydroxide (typical concentration 23–35 wt%; pH about 14–15). Schematically the process can be represented as in Fig. 1. A potential difference between the cathode and the anode is sustained (about 2–4 V) in such a way that the desired current density is obtained (typically 2000–5000 A/m²). The surface of the membrane is about 1–3 m². The membrane cell units as sketched in Fig. 1 are serially coupled in a so-called stack where about 20 to more than 100 of these (independently working) units are present. The membranes used in the chloralkali electrolysis process are cation selective membranes. The membranes are made of a crosslinked polymeric network on which functional groups are fixed. In the membranes used in the chloralkali industry two types of active groups are attached to the matrix: carboxylic groups ($-\text{CO}_2^-$) and sulfonic groups ($-\text{SO}_3^-$). The transport and sorption properties of a specific layer can be adjusted by the number of moles of active groups per kilogram dry polymer (which is the reciprocal value of the so-called *equivalent weight*). The membranes used in the chloralkali industry are composite membranes, i.e., they consist of a serial combination of sulfonic and carboxylic layers in order to obtain the desired performance properties. The sulfonic layer is reinforced with Teflon wires to increase the mechanical stability of the membrane. The sulfonic layer is mostly placed at the anode side of the electrolysis cell in order to prevent the protonation of the carboxylic groups in the carboxylic layer which could occur in the relatively acidic

environment as present in the anode compartment. If the protonation of the carboxylic layer would occur, the resistance in the carboxylic layer would increase drastically. By means of a small pressure difference (about 0.1 bar) between the anode and cathode compartment, the membrane is pressed against the anode. This has been done to decrease the mass transfer from the anode to the membrane, where due to the lower electrolyte concentration, the electrical resistance is larger than in the catholyte compartment. The distance between the cathode and the membrane is about 1 mm. The anode has a mesh structure, while the cathode is a perforated plate with holes of about 1 mm. The electrolysis process is carried out at near atmospheric pressures and at a temperature of 80–95°C in order to increase the conductivity of the electrolyte solution, and therewith decrease the power consumption.

Over the last 10 yr AKZO-Nobel among others has obtained a lot of experimental data with membranes of DuPont (trade name Nafion), Asahi Chemical (Aciplex) and Asahi Glass (Flemion) not only in the industrially used electrolyser but also in a pilot plant. The pilot plant electrolyser was used in order to obtain experimental data for various operating conditions. The pilot plant cell was, apart from the size, completely identical to the industrially used electrolyzers of AKZO-Nobel as used in, e.g., Rotterdam, The Netherlands. The total cell potential and also the fluxes of all relevant species have been measured which enables the determination of important parameters as the Current Efficiency (CE = the percentage of the current which is transported by Na^+), the water transport number (t_w = the number of moles of water transported per mole of Na^+ transported).

For a reliable theoretical prediction of these performance parameters a suitable mass transfer model must be used. This mass transfer model must be complemented with a model able to predict equilibria at the various liquid–membrane and membrane–membrane interfaces. van der Stegen et al. (1998a) have presented a mass transfer model based on the Maxwell–Stefan theory and applicable to ion-selective membranes. In another study by van der Stegen et al. (1998b) an equilibrium model, based on the Pitzer equilibrium model, was presented which can be used to calculate the equilibrium composition at the various liquid–membrane and membrane–membrane interfaces. A combination of the mass transfer model and the equilibrium model basically enables the prediction of the performance of the chloralkali electrolysis process once the required parameters like, among others, Maxwell–Stefan diffusivities are available. In this study the predictions according to the mass transport model are compared to the experimental results of Akzo-Nobel obtained in the pilot plant electrolyser with the Nafion membrane of DuPont.

2. Application of the maxwell-stefan theory to the membrane electrolysis process

In this section the transport equations based on the Maxwell–Stefan theory are summarized which are necessary for the description of the mass transfer in the membrane electrolysis cell. In the model the charged groups of the membrane are assumed to behave similarly as the ionic components in the aqueous electrolyte solution. The membrane charged groups are kept in place by some external clamping force. The mass transport equations which were derived for the transport in ion-selective membranes in a previous paper are (van der Stegen, 1998a):

- $n - 2$ independent Maxwell–Stefan equations for component 1 to $n - 2$:

$$(N) = [A](\nabla x) - [\beta]x \quad (1)$$

in which N is the matrix with the $(n - 2)$ fluxes with respect to the (stationary) membrane.

- Two supplementary equations for component $n - 1$ and n :

$$\sum_{i=1}^n z_i x_i = 0, \quad i = n - 1, \quad (2)$$

$$\sum_{i=1}^n x_i = 1, \quad i = n. \quad (3)$$

For the contents of the matrices A and β the reader is referred to Appendix A. These matrices contain, among others, the current density and the Maxwell–Stefan diffusivities. In a mixture containing n components $0.5n(n - 1)$ Maxwell–Stefan diffusivities are needed to take into account the interaction between all species. At the same time, this is currently the bottleneck in the application of the Maxwell–Stefan theory to the membrane: very little information is available on the values of these diffusivities. The method used to obtain the diffusivities is outlined in Section 3. Before the mass transfer model can predict accurate transport data, the boundary conditions at each mass transfer layer must be determined also. For this an appropriate equilibrium model is necessary. In a previous paper (Stegen, 1998b) it was shown that the modified Pitzer model can be used to predict these equilibria for the sulfonic layer of a DuPont Nafion membrane with equivalent weights of 1100 and 1500. In the same way as for the sulfonic layer the parameters according to the modified Pitzer model have also been determined for the carboxylic layer in the DuPont Nafion membrane. However, for reasons of confidentiality the measured sorption data cannot be presented: only the resulting Pitzer parameters which were derived from these sorption measurements received clearance for publication (see Appendix B).

Table 1

Classification of the Maxwell–Stefan diffusivities which have to be known in each separate phase

	Positive ions	Negative ions	Water
Membrane	$D_{+,m}$ ($D_{Na^+,m}$)	$D_{-,m}$ ($D_{Cl^-,m}, D_{OH^-,m}$)	$D_{w,m}$
Water	$D_{+,w}$ ($D_{Na^+,w}$)	$D_{-,w}$ ($D_{Cl^-,w}, D_{OH^-,w}$)	—
Negative ions	$D_{+,-}$ ($D_{Na^+,Cl^-}, D_{Na^+,OH^-}$)	$D_{-,-}$ (D_{Cl^-,OH^-})	
Positive ions	$D_{+,+}$ Not relevant: only 1 type of + ion present		

3. Determination of Maxwell–Stefan diffusivities for the chloralkali electrolysis process from literature

As already mentioned an important limitation in the application of the Maxwell–Stefan theory to the membrane is the present lack of accurate Maxwell–Stefan diffusivities inside the membrane. For a multicomponent system with n components $1/2n(n - 1)$ Maxwell–Stefan diffusivities $D_{i,j}$ are required. These binary diffusivities are a measure for the interaction between each component i with another component j in the mixture. A distinction should be made between the diffusivities in the free solution and the membrane phase. The diffusivities in the free solution can (partially) be found in open literature, however, for the membrane phase no diffusivities are available. It is important to emphasize that the membrane can consist of different layers, each with its own transport properties.

So, it is obvious that the number of diffusivities, which have to be known for a correct description of the overall mass transfer process, can be very high. In Table 1 the various types of Maxwell–Stefan diffusivities which affect the performance of a membrane in the chloralkali electrolysis are schematically represented. In this scheme only the main components in the chloralkali electrolysis process have been taken into account, i.e., the membrane charged groups, water, sodium, chloride and hydroxide respectively.

Wesselingh et al. (1995) have presented some methods to estimate the values of these diffusivities in the membranes, the method being partially based on the values of the diffusivities in the free solution. However, application of the method suggested by Wesselingh et al. (1995) for the standard conditions of the chloralkali electrolysis process (see Table 6) led to a potential drop over the membrane of several volts. This was much higher than the experimentally observed tenths of a Volt, indicating that the estimated diffusivities were much too low. Therefore, another method had to be applied in order to estimate the diffusivities inside the membrane.

Table 2

Process conditions of the 'standard' experiment, which resembles the conditions at normal operation

Component	Anolyte [mole fraction]	Catholyte [mole fraction]
Cl ⁻	0.05466	2.033×10^{-5}
OH ⁻	0	0.10602
Na ⁺	0.05466	0.10604
H ₂ O	0.89066	0.78793
NaCl-anolyte (g/l)	180	
NaOH-catholyte (wt%)	23	
current density (A/m ²)	4000	
Current efficiency (%)	94.5	
Water transport number (mol/F)	4.6	
ΔV_{cell} (V)	3.49	
Temperature [°C]	90	

Table 3

Degree of influence of the various diffusivities

Important	Unimportant
$D_{\text{OH}^-, \text{w}}$	$D_{\text{Cl}^-, \text{m}}$
$D_{\text{OH}^-, \text{Na}^+}$	$D_{\text{OH}^-, \text{m}}$
$D_{\text{Na}^+, \text{m}}$	$D_{\text{Cl}^-, \text{w}}$
$D_{\text{Na}^+, \text{w}}$	$D_{\text{Cl}^-, \text{OH}^-}$
$D_{\text{m}, \text{w}}$	$D_{\text{Cl}^-, \text{Na}^+}$

4. Determination of maxwell–stefan diffusivities for the chloralkali electrolysis process from experiments

First a sensitivity analysis was carried out, in order to reduce the set of diffusivities as shown in Table 1 by determining the dominating diffusivities. The process conditions were taken as the standard process conditions during the electrolysis process (see Table 2), and the membrane was given the (sorption) properties of the sulfonic layer of the DuPont Nafion membrane with an equivalent weight of 1500 (see Appendix B). All diffusivities were initially taken at a value of 1×10^{-9} m²/s. Subsequently, the value of one of the diffusivities was lowered and the effect on the fluxes of all components was observed. Only the diffusivities which had a substantial influence on more than 1 flux were considered as the 'important' diffusivities (see Table 3). However, if the set of 'important' diffusivities from Table 3 would be selected, it would be impossible to describe the Cl⁻ flux. Therefore, one extra diffusivity ($D_{\text{Cl}^-, \text{m}}$) was incorporated in the set in order to describe the Cl⁻ flux also correctly. The remaining set of diffusivities and their influence on the various fluxes are summarized in Table 4. In the subsequent simulations carried out and reported in this paper the diffusivities not occurring in Table 4 were given an arbitrarily chosen relatively large value of 1×10^{-8}

Table 4

Remaining set of Maxwell-Stefan diffusivities and their influence

Diffusivity	Affects mainly flux of	Remarks
$D_{\text{OH}^-, \text{w}}$	OH ⁻ , H ₂ O, Na ⁺ , Cl ⁻	To determine the order of magnitude of the fluxes
$D_{\text{Na}^+, \text{w}}$	H ₂ O	To adjust the H ₂ O-flux
$D_{\text{w}, \text{m}}$	OH ⁻ , H ₂ O, Na ⁺ , Cl ⁻	To determine the order of magnitude of the fluxes
$D_{\text{OH}^-, \text{Na}}$	OH ⁻	To adjust the OH ⁻ -flux
$D_{\text{Na}^+, \text{m}}$	OH ⁻ , H ₂ O, Na ⁺ , Cl ⁻	To determine the order of magnitude of the fluxes
$D_{\text{Cl}^-, \text{m}}$	Cl ⁻	To adjust the Cl ⁻ -flux

Table 5

Fitted values of the diffusivities on experimental results for single membrane layers

Diffusivity (m ² /s)	Single sulfonic layer	Single carboxylic layer
$D_{\text{OH}^-, \text{w}}$	1.0×10^{-9}	4.5×10^{-10}
$D_{\text{Na}^+, \text{w}}$	9.0×10^{-10}	6.0×10^{-10}
$D_{\text{w}, \text{m}}$	1.0×10^{-9}	1.0×10^{-10}
$D_{\text{OH}^-, \text{Na}}$	1.0×10^{-9}	2.6×10^{-10}
$D_{\text{Na}^+, \text{m}}$	1.17×10^{-10}	1.0×10^{-9}
$D_{\text{Cl}^-, \text{m}}$	1.0×10^{-10}	1.0×10^{-11}

Note: Experimental results for the single membrane layers taken from Yeager et al. (1982a–c) (Conditions used by Yeager et al.: $T = 80^\circ\text{C}$; $\text{CD} = 2000 \text{ A/m}^2$; $\text{EW}_{\text{sulfonic}} = 1150$; $\text{EW}_{\text{carboxylic}} = 1260$).

Table 6

Physical properties of the DuPont Nafion membrane as used

Layers	Sulfonic	Carboxylic
EW (g/mol)	1015	1619
Density (kg/m ³)	1640	1640
Thickness (dry) (μm)	60	20

m²/s so that they did not have any limiting influence at all. The values for the set of the diffusivities in Table 4 was estimated from experimental results reported in literature for *single* layer carboxylic as well as sulfonic membranes (Yeager et al., 1982a–1982c). These resulting diffusivities are given in Table 5. The diffusivities from Table 5 were taken as the starting point for the determination of the diffusivities in the actual sulfonic and carboxylic layer as present in the DuPont Nafion membrane. The diffusivities as given in Table 5 could not be used directly for this membrane, because the properties of the single sulfonic and carboxylic membranes differ from the properties of the layer in the DuPont Nafion membrane (Tables 5 and 6). Also the process conditions as used in the experiments with the single layer membranes differ from the process conditions those used usually by AKZO-Nobel (see Tables 2 and 5).

Table 7
Fitted diffusivities for the reference experiment for the DuPont Nafion membrane

Diffusivities (m^2/s)	Sulfonic	Carboxylic
$D_{\text{OH},w}$	1.0×10^{-9}	8.0×10^{-10}
$D_{\text{Na},w}$	1.1×10^{-9}	1.1×10^{-9}
$D_{w,m}$	1.0×10^{-9}	6.5×10^{-10}
$D_{\text{OH},\text{Na}}$	1.0×10^{-9}	3.0×10^{-10}
$D_{\text{Na},m}$	3.0×10^{-10}	1.0×10^{-9}
$D_{\text{Cl},m}$	1.0×10^{-11}	6.0×10^{-13}

The diffusivities as determined for the single layer membranes (Table 5) were adapted in such a way that for the DuPont Nafion membrane the experimentally observed fluxes were attained. In this procedure the influence of a change in the diffusivities in the carboxylic layer turned out to be of much more influence than a change of the diffusivities in the sulfonic layer. The reason for this is that the diffusivities in the carboxylic layer are considerably lower and therefore have a much larger impact on the performance than the diffusivities in the sulfonic layer. The resulting fine tuned diffusivities for the DuPont Nafion membrane are given in Table 7 and are approximately a factor 5–100 higher than the diffusivities predicted according to the methods given in the paper of Wesselingh et al. (1995). Now, for the experimental conditions as presented in Table 2 (the ‘standard conditions’), the predicted fluxes differed by no more than a few percent from the experimentally measured fluxes. This means that also the current efficiency and water transport number are nearly identical to those observed ex-

perimentally. In Fig. 2 the calculated mole fraction profiles over the membrane are given, while in Fig. 3 the log $[\text{OH}^-]$ and the potential profile are given. As can be seen in Fig. 2 the mole fraction profiles are nearly constant in the (thick) sulfonic layer, while in the carboxylic layer steep mole fraction gradients occur. This indicates that the major mass transfer resistance is located in the thin carboxylic layer. This could also be expected because the diffusivities determined for the carboxylic layer are considerably lower than for the sulfonic layer. The change of the mole fraction of the membrane in the carboxylic layer suggests that the concentration of its charged groups varies considerably over this layer, which may seem rather peculiar. However, if the mole fraction is converted to concentrations, the concentration of the membrane charged groups remains nearly constant over the whole carboxylic layer (profile is not shown). If the log $[\text{OH}^-]$ profile as depicted in Fig. 3 is studied, it can be seen that this value rapidly increases just inside the sulfonic layer at the anolyte side. At a low value of the pH the carboxylic membrane may be protonated, resulting in a very high (electrical) resistance and loss of the selectivity. According to Yeager (1982a), protonation of the carboxylic layer starts at a pH value of about 4 and has a major effect on the ability of Na^+ to diffuse through the polymer matrix. Moreover, in industry, acid is even added to the anode compartment which could result in a pH value of less than 2. Adding a sulfonic layer prevents the possible protonation of the carboxylic layer which would result in a very large mass transfer resistance in the carboxylic layer. In Fig. 3 also the calculated potential profile is given, and from this profile again it can be concluded that the largest resistance is located in the

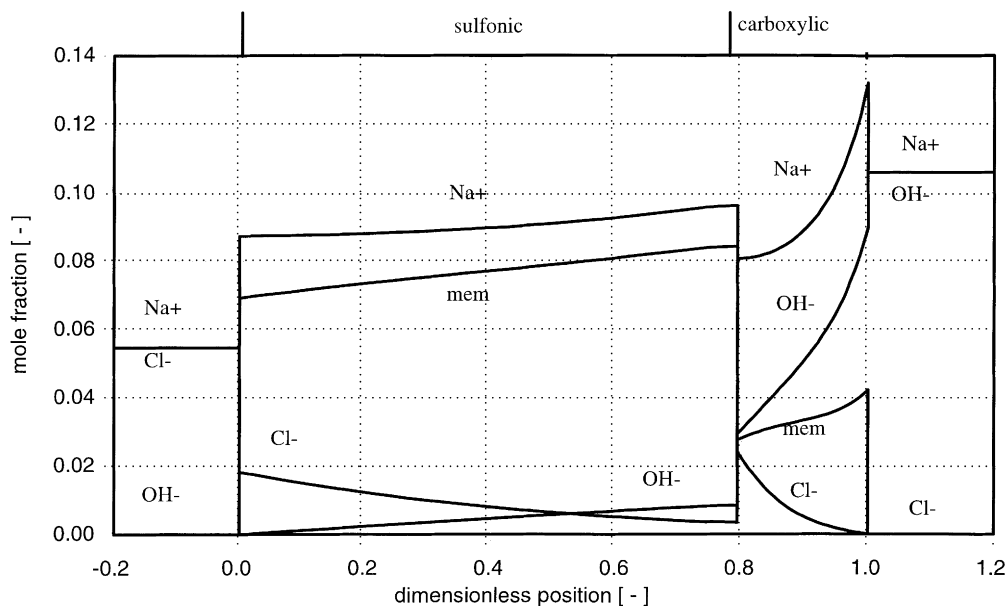


Fig. 2. Mole fraction profile in the DuPont Nafion membrane for the reference experiment (see Table 2).

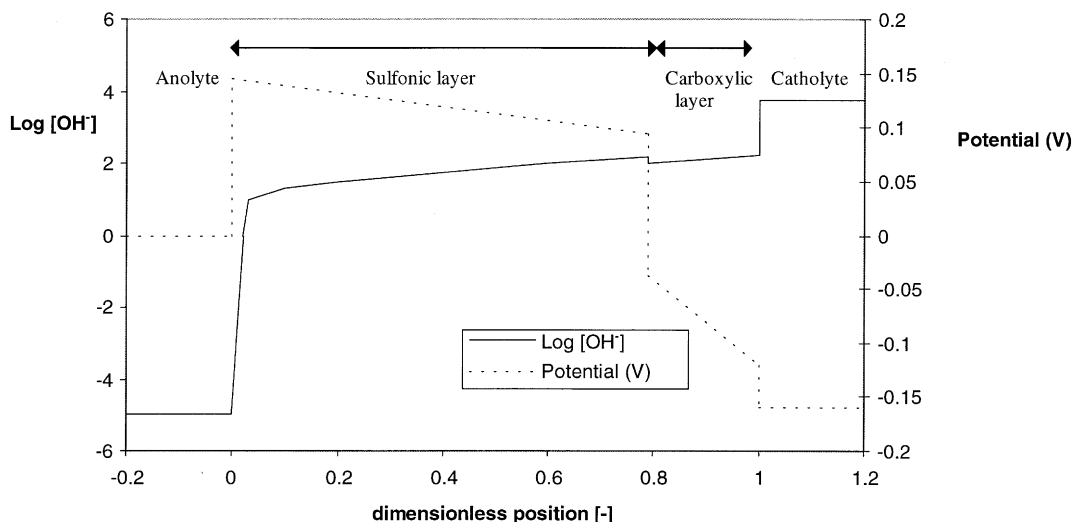


Fig. 3. Calculated $\log [\text{OH}^-]$ profile and potential profile in the DuPont Nafion membrane for the reference experiment (see Table 2). The potential in the anolyte was given a reference potential of 0 V.

relatively thin carboxylic layer. The value of calculated potential drop over the membrane could not be compared to experiments, because in the experiments only the total cell potential was determined ($\pm 3\text{--}4\text{ V}$), which is the sum of the potential drops at both electrodes (including the over potential), in the cathode solution and anode solution and in the membrane. As compared to the total cell potential the membrane potential drop is only about 15% of the total cell potential.

5. Application of the Maxwell–Stefan model

The model has been applied to the standard conditions and the values of the diffusivities have been determined for these conditions. It is interesting to study whether this set of diffusivities is also valid for other than the standard conditions. In this section the simulations of the model for non-standard conditions will be presented. The anolyte strength, the catholyte strength and the current density will be varied with respect to the standard conditions as given in Table 2.

5.1. Variation of the anolyte strength

The same values of the diffusivities as obtained for the reference experiment (see Tables 2 and 7) were used to simulate the experiments with other anolyte strengths. Fig. 4 shows the theoretical and experimental performance indicators of the process like current efficiency and water transport number (the reference experiment is always marked with a '□'). As can be seen in Fig. 4 the model predicts the experimental current efficiency reasonably well, while the water transport number is predicted very accurately.

5.2. Variation of the catholyte strength

With the same set of diffusivities as for the reference experiment (see Table 7), the experiments with varying catholyte strength were simulated. The results of the calculations are presented in Fig. 5. As can be seen in Fig. 5, the results for the current efficiency are completely out of line with the experimentally observed behavior. If the catholyte concentration is increased, two opposing effects occur:

- The driving force for the OH^- -ion to diffuse to the anode side increases (increase of the mole fraction gradient) which results in a higher molar flux of OH^- . This effect is incorporated in the transport model.
- The water uptake of the carboxylic layer decreases with an increase in the salt concentration (due to a lower water activity, see van der Stegen (1995)). Therefore the 'porosity' of the carboxylic layer decreases which results in a higher friction (tortuosity) inside the membrane (Wesselingh et al., 1995) and a lower flux of OH^- . In the model this variation of the friction of (one of the) components is not incorporated. In order to take this effect into account some modification of the diffusivities is required.

Wesselingh et al. (1995) suggested the following relation between the diffusivity and the tortuosity τ .

$$D_{i,j} = D_{i,j}^{\text{free solution}} \tau \quad \text{with} \quad \tau = \xi^{1.5}. \quad (4)$$

The tortuosity is a function of the water uptake ξ . The water uptake is defined as:

$$\xi = \frac{\text{m}^3 \text{ sorbed solvent}}{\text{m}^3 \text{ swollen membrane}}. \quad (5)$$

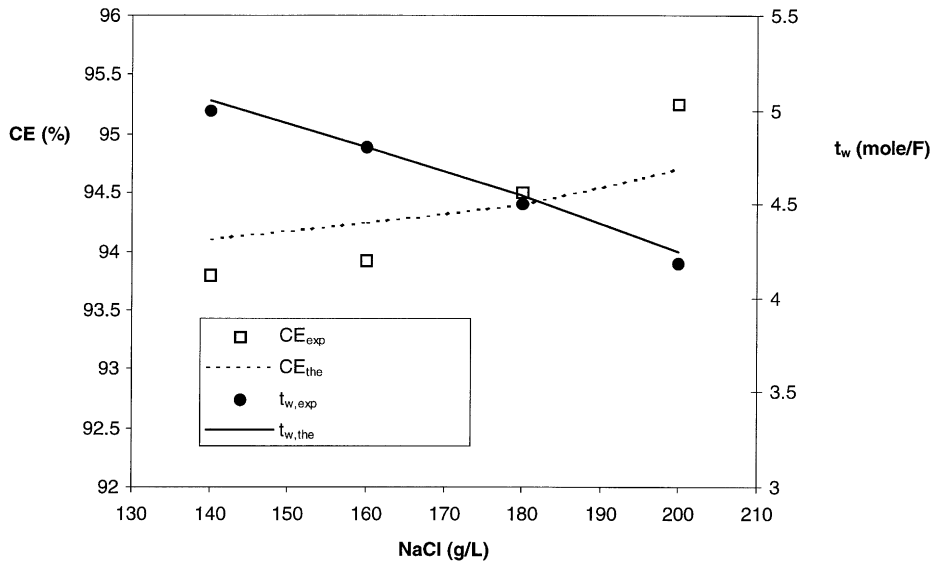


Fig. 4. Experimental and theoretical performance indicators for the DuPont Nafion membrane for varying anolyte strengths.

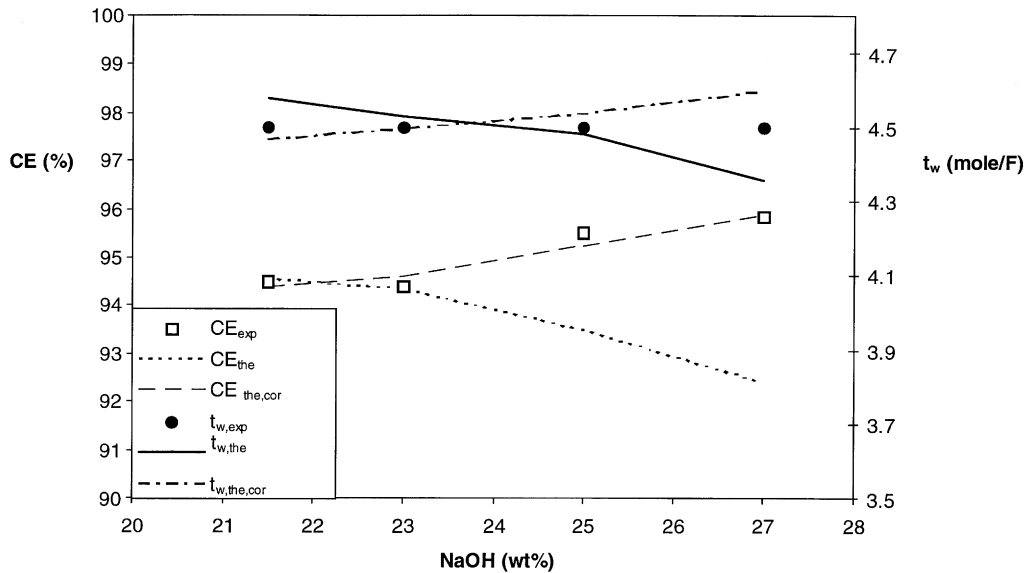


Fig. 5. Experimental and theoretical performance indicators for the DuPont Nafion membrane with and without a correction of the $D_{carboxylic}$ for the catholyte strength (see also Fig. 6).

To correct the diffusivities for the water uptake, only the values of the diffusivities for the carboxylic membrane have to be changed, because it is unlikely that the water uptake of the sulfonic layer does change considerably (considering it is exposed to the anolyte). Moreover, the influence of the sulfonic layer on the transport is limited as shown in Section 4. The values of the diffusivities for the carboxylic layer were corrected for the water uptake with respect to the 'standard' experimental conditions (Table 2). The correction factor (change in the tortuosity with respect to the free solution) is calculated according to Eq. (6) in which the reference experiment

has a correction factor equal to one.

$$\text{correction factor} = \left(\frac{\xi}{\xi_{\text{reference experiment}}} \right)^{1.5}. \quad (6)$$

The water up-take for the carboxylic layer was calculated with the relation as determined by van der Stegen (1989) for a carboxylic membrane:

$$\xi = 1.045 + 0.3272\gamma_w + 0.1343\gamma_w^2 - 1.496EW + 0.55EW^2 - 0.28922\gamma_w EW. \quad (7)$$

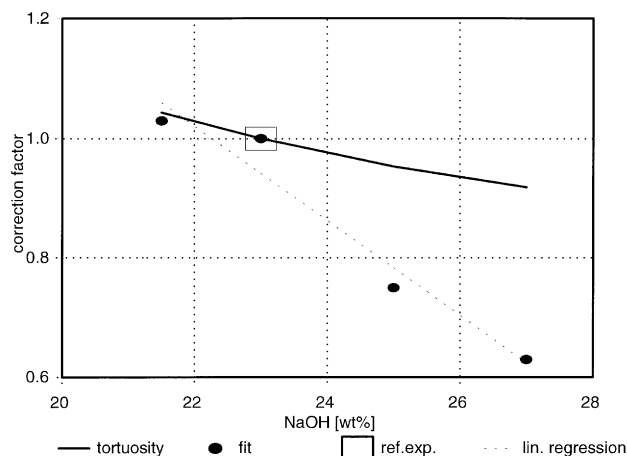


Fig. 6. Fitted correction factor and correction factor (tortuosity) for $D_{\text{carboxylic}}$ obtained from the water uptake.

Simulations showed that this adjustment of the values of the dominating diffusivities (Table 3) resulted in an increase of the current efficiency with an increasing catholyte strength, but this adaptation was not sufficient to obtain the correct value of the current efficiency. Therefore the correction factor was fitted to meet the experimentally observed Na^+ and OH^- fluxes. The fitted correction factor and the correction factor obtained from the water uptake (tortuosity) is given in Fig. 6. This figure shows that the proposed dependency of the water uptake is insufficient. As it is not known whether other phenomena affect the diffusivities the application of relations like Eq. (6) is questionable. Linear regression results in

the following relation for the correction of all the diffusivities for the carboxylic layer:

$$D_{\text{carboxylic}} = D_{\text{carboxylic}}^{\text{ref.exp}} (-16.748x_{\text{OH}}^{\text{cathode}} + 2.7174). \quad (8)$$

Fig. 5 also presents the experimental and theoretical performance indicators for varying catholyte strengths obtained with the diffusivity $D_{\text{carboxylic}}$ estimated according to the empirically determined Eq. 8. From Fig. 5 it can be concluded that the experimental current efficiency can be obtained by including an empirical correction factor for $D_{\text{carboxylic}}$. Of course, for the reference experiment the correction factor is equal to 1. The water transport number is also reasonably well predicted.

5.3. Variation of the current density

The same diffusivities as obtained for the reference experiment (see Table 7) were used to simulate the performance of the DuPont Nafion membrane at lower current densities. The results of the calculations are shown in Fig. 7. As can be seen in Fig. 7 the correct trends in the performance indicators are predicted by the model. The current efficiency and the water transport number decrease with the current density, but the model predicts a much more pronounced behaviour. However, from experimental observations (Nakao et al., 1997) for a similar membrane (Asahi Glass 893 membrane) it was shown that the water content inside the membrane decreases with the current density. This implies higher friction at lower current densities and therefore the necessity for a correction factor for the values of the important diffusivities (sulfonic and carboxylic). In Fig. 8 the correction factor is given for the diffusivities D to meet the

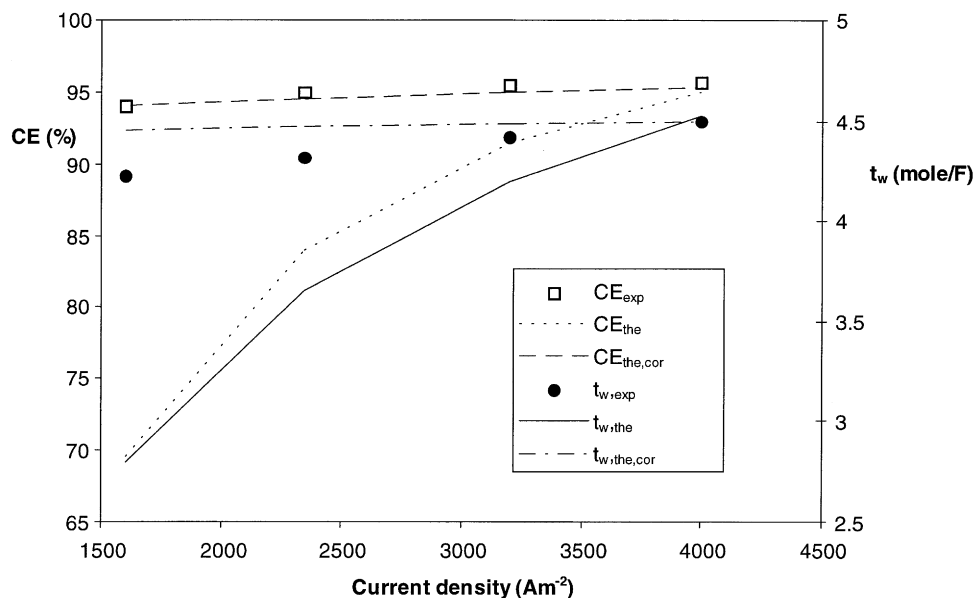


Fig. 7. Experimental and theoretical performance indicators for the DuPont Nafion membrane with and without correction of the diffusivities D for the current density (see also Fig. 8).

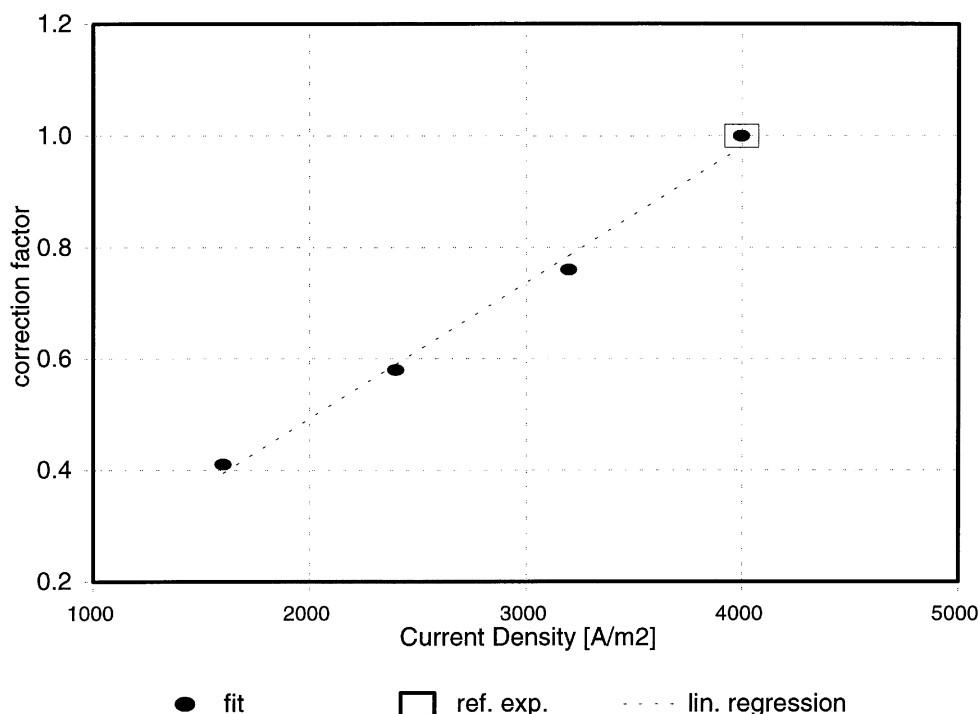


Fig. 8. Correction factor for the diffusivities \bar{D} in the carboxylic and sulfonic layer in the DuPont Nafion membrane.

experimental current efficiency. For the sulfonic as well for the carboxylic layer, the same correction factor was applied. Linear regression results in the following relation for the correction of the values of the diffusivities for the current density I (sulfonic and carboxylic):

$$\bar{D} = (2.4423 \times 10^{-4}I + 0.037)\bar{D}^{\text{ref. exp.}} \quad (9)$$

Fig. 7 also shows the experimental and theoretical current efficiency and water transport number obtained with the correction of the diffusivities for the current density. The current efficiency is well predicted by using this correction, but the simulation of the water transport number results in slightly higher values at low current densities.

6. Discussion and conclusions

To obtain reliable values for the membrane diffusivities for the DuPont Nafion membrane, first the method presented by Wesselingh et al. (1995) was used. This method gave too low values for the diffusivities and therewith an unrealistic high membrane potential drop. Therefore, another method was followed. First, a sensitivity analysis was carried out which resulted in a reduced set consisting of the dominating Maxwell–Stefan diffusivities. First estimates of these remaining diffusivities were determined for single layer sulfonic and a carboxylic membranes. With a slight adjustment of the values of the diffusivities obtained for the separate sul-

fonic and carboxylic layers, the performance parameters of the DuPont Nafion membrane could be predicted well for the standard conditions. These diffusivities also proved to be suitable for other anolyte strengths. However, for other catholyte strengths and current densities these diffusivities (even after a correction for the water uptake according to the method of Wesselingh et al. (1995)) did not result in a good agreement between the simulated and experimentally observed performance parameters and a correction factor had to be introduced. From this it can be concluded that although a fundamental model is used in order to describe the mass transfer in a membrane, a single set of diffusivities, even with a correction for the water uptake according to the method of Wesselingh et al. (1995), is not sufficient in order to obtain the experimentally observed performance parameters. At this moment there is not enough knowledge on the exact phenomena taking place in the membrane in order to predict the required corrections of the diffusivities a priori. Therefore in this paper these correction factors were empirically derived.

This study indicates that the (the methods to determine the) Maxwell–Stefan diffusivities for the membrane phase as reported in literature are not suitable for the prediction of the transport through a membrane during chloralkali electrolysis conditions. Application of the (reduced) set of diffusivities and the correction factors for them, gives a reasonably good agreement between the theoretical and experimental results but is strictly speaking only applicable for the conditions as used in this

study. With the derived set of Maxwell–Stefan diffusivities it is possible to estimate the performance of the membrane at other thicknesses of both the sulfonic and carboxylic layer, current density and catholyte and anolyte strength. Also the calculated mole fraction and potential profiles across the membrane are very helpful in the understanding of the behavior of the membrane, which may contribute to the further improvement of the characteristic properties of the membrane. As long as there are no theoretically founded and reliable relations available to predict the Maxwell–Stefan diffusivities in a membrane (or accurate experimental data for these diffusivities) only a method as used in this study can serve as a basis for a further progress in the development of an existing (in this case DuPont Nafion) membrane.

Notations

A	matrix with non-idealities, transference numbers and diffusivities
B^{n*}	matrix with diffusivities
c_T	total concentration mol/m ³
C^ϕ	Pitzer interaction parameter
CE	current efficiency %
D	Maxwell–Stefan diffusivity m ² /s
EW	equivalent weight of the membrane layer g/mol
$f_{\text{shielding}}$	correction factor for the equivalent weight
F	Faraday constant (= 96487) C/mol
I	current density A/m ²
K	equilibrium constant
n	total number of components
N	molar flux mol/m ² /s
p	pressure Pa
R	universal gas constant (8.314413) J/mol K ⁻¹
t_w	water transport number mol/F
T	temperature K
V	molecular volume m ³ /mol
x	mole fraction
z	ionic charge
$Z^\#$	matrix with electrical coefficients

Greek letters

β	matrix consisting of B^{n*} and $Z^\#$
β^0, β^1	Pitzer dependent parameter
γ	activity coefficient
ΔV	potential drop V
κ	conductivity of the ionic solution Ω^{-1}/m
Ξ	matrix with thermodynamic non-idealities and transference numbers
ξ	water uptake m ³ _{water} m ³ _{membrane}
Φ	Pitzer interaction parameter
ψ	Pitzer interaction parameter
τ	tortuosity

Appendix A. Model equations

Matrix A contains diffusivities, thermodynamic non-idealities and transference numbers:

$$[A] = [B^{n*}]^{-1}[\Xi^*]. \quad (\text{A.1})$$

The matrix $[A]$ can be split into two parts:

- a matrix with diffusivities $[B^{n*}]$
 - a matrix with thermodynamic non-idealities and transference numbers $[\Xi^*]$
- and matrix β with diffusivities and the current density:

$$[\beta] = [B^{n*}]^{-1}[Z^\#]. \quad (\text{A.2})$$

The different matrices are defined as follows:

- Matrix with diffusivities $[B^{n*}]$:

$$B_{i,j}^{n*} = B_{i,j}^n - B_{i,n-1}^n \frac{z_j}{z_{n-1}}, \quad i = 1, \dots, n-2, \quad (\text{A.3})$$

with

$$B_{i,i}^{n*} = -\frac{1}{c_T} \sum_{\substack{k=1 \\ k \neq i}}^n \frac{x_k}{D_{i,k}} \quad (\text{A.3a})$$

$$B_{i,j}^n = \frac{x_i}{c_T D_{i,j}} \quad i \neq j. \quad (\text{A.3b})$$

- Matrix with thermodynamic non-idealities and transference numbers $[\Xi]$:

$$\Xi_{i,j}^* = \Xi_{i,j} - \Xi_{i,n-1} \frac{z_j - z_n}{z_{n-1} - z_n}, \quad i = 1, \dots, n-2, \quad (\text{A.4})$$

$$j = 1, \dots, n-2,$$

with

$$\Xi_{i,j} = \Gamma_{i,j} - x_i z_i \sum_{k=1}^{n-1} \Gamma_{k,j} \frac{t_k^n}{z_k x_k}, \quad (\text{A.4a})$$

$$\Gamma_{i,j} = \delta_{i,j} + x_i \left. \frac{\partial \ln \gamma_i}{\partial x_j} \right|_{T,P,x_k, k \neq j=1, \dots, n-1}, \quad (\text{A.4b})$$

$$t_j^n = \frac{z_j x_j c_T^2 F^2}{\kappa} \sum_{k=1}^{n-1} L_{j,k}^n z_k x_k \quad (\text{A.4c})$$

$$\kappa = c_T^2 F^2 \sum_{i=1}^{n-1} \sum_{j=1}^{n-1} z_i z_j x_i x_j L_{i,j}^n, \quad (\text{A.4d})$$

$$[L^n] = -[M^n]^{-1}. \quad (\text{A.4e})$$

$[M^n]$ follows from $[M]$ in which the n th row and column have been removed:

$$M_{i,j} = K_{i,j}, \quad i \neq j = 1, 2, \dots, n, \quad (\text{A.4f})$$

$$M_{i,i} = K_{i,i} - \sum_{k=1}^n K_{i,k}, \quad i = 1, 2, \dots, n \quad (\text{A.4g})$$

$$K_{i,j} = RT \frac{x_i x_j c_T}{D_{i,j}}. \quad (\text{A.4h})$$

Table 8
Pitzer interaction parameters at 90°C for the sulfonic and carboxylic layer of the DuPont Nafion membrane

Interaction parameter	Sulfonic	Carboxylic
$\beta_{\text{Na}^+}^{(0)}, \text{ membrane}$	0.07031	− 0.2874
$\beta_{\text{Na}^+}^{(1)}, \text{ membrane}$	− 11.0268	0
$C_{\text{Na}^+}^{(0)}, \text{ membrane}$	− 0.00362	0.02202
$\phi_{\text{Cl}^-}, \text{ membrane}$	0.28584	0
$\Psi_{\text{Na}^+, \text{Cl}^-}, \text{ membrane}$	− 0.04446	1.52×10^{-3}
$\phi_{\text{OH}^-}, \text{ membrane}$	0.17011	0.2458
$\Psi_{\text{Na}^+, \text{OH}^-}, \text{ membrane}$	− 0.01134	− 0.02026

● Matrix with diffusivities and current density $Z^\#$:

$$Z_{i,j}^\# = 0, \quad i \neq j = 1, 2, \dots, n-2, \quad (\text{A.5a})$$

$$Z_{i,i}^\# = \left(\frac{z_i F}{RT\kappa} + \frac{1}{F c_T D_{i,n-1} z_{n-1}} \right) I, \quad i = 1, 2, \dots, n-2. \quad (\text{A5b})$$

Appendix B. pitzer parameters

In this Appendix the Pitzer parameters for the sulfonic and carboxylic layer in the DuPont Nafion membrane are given. The data for the sulfonic layer were taken from the paper of van der Stegen et al. (1998b). The symbols are in accordance with the symbols used by Pitzer (1991) and van der Stegen et al. (1991). In both references also the Pitzer relations and other relevant Pitzer parameters are given (Table 8).

The data mentioned are valid for an equivalent weight of $\text{EW}_{\text{sulfonic}} < 1100 \text{ g/mol}$ and $\text{EW}_{\text{carboxylic}} < 1100 \text{ g/mol}$. In order to apply it to the membrane as used in this study ($\text{EW}_{\text{sulfonic}} = 1015 \text{ g/mol}$ and

$\text{EW}_{\text{carboxylic}} = 1609 \text{ g/mol}$), the shielding factor ($= f_{\text{shielding}}$ introduced by van der Stegen et al. (1998b)) for the sulfonic and carboxylic layer should be taken at $f_{\text{shielding, sulfonic}} = 1$ and $f_{\text{shielding, carboxylic}} = 0.096$, respectively.

References

- Kraaijeveld, G. (1994). *The Maxwell–Stefan description of mass transfer in ion exchange and electrodialysis*. Ph.D. thesis, Rijksuniversiteit Groningen.
- Nakao, M., Shimohira, T., & Takechi, Y. (1997). High performance operation with Flemion membranes and the AZEC-B1 electrolyzer. Paper presented at the *Chlorine Symposium in London*, April 1997.
- Pitzer, K.S. (1991). *Activity coefficients in electrolyte solutions* (2nd ed.). Boston: CRC Press.
- Stegen van der, J.H.G., Weerdenburg, H., Veen van der, A.J., Hogendoorn, J.A., & Versteeg, G.F. (1998a). Application of the Maxwell–Stefan theory to the membrane electrolysis process: Model development and simulations. Submitted.
- Stegen van der, J.H.G., Veen van der, A.J., Weerdenburg, H., Hogendoorn, J.A., & Versteeg, G.F. (1998b). Application of the Pitzer model for the estimation of activity coefficients of electrolytes in ion selective membranes. *Fluid Phase Equilibria*, accepted.
- Stegen van der, J.H.G. (1989). Internal Akzo-Nobel Report No. 89.00.440.
- Taylor, R., & Krishna, R. (1993). *Multicomponent mass transfer* (Ch. 1 and 2). New York: Wiley.
- Wesselingh, J.A., Vonk, P., & Kraaijeveld, G. (1995). Exploring the Maxwell–Stefan description of ion exchange. *Chem. Engng J.*, 57, 75–89.
- Yeager, H.L., Twardowski, Z., & Clarke, L.M. (1982a). A comparison of perfluorinated carboxylate and sulfonate ion exchange polymers. 1. Diffusion and water sorption 2. Sorption and transport properties in concentrated solution environments. *J. Electrochem. Soc.*, 129(2), 324–332.
- Yeager, H.L., O'Dell, B., & Twardowski, Z. (1982b). Transport properties of nafion membranes in concentrated solution environments. *J. Electrochem. Soc.*, 129(1), 85–89.
- Yeager, H.L., Kipling, B., & Datson, R.L. (1982c). Sodium ion diffusion in nafion ion exchange membranes. *J. Electrochem. Soc.*, 127(2), 303–307.